Computational study of phytocompounds derived from *Glycine max* as potential inhibitors of Estrogen Receptor alpha of breast cancer

Golam Gaus Mohiuddin
Noakhali Science and Technology University
Mohammad Mahfuz Enam Elahi
University of Asia Pacific
Md. Jahed Rana
State University of Bangladesh
Md. Al Hafiz
Kennesaw State University
Kaniz Fatema
Jahangirnagar University
Abir Hossain
University of Dhaka
Md. Shohel Hossain
Gono University
Nigar Sultana
Noakhali Science and Technology University
Md. Saddam Hussain
Noakhali Science and Technology University
Mohammad Safiqul Islam
research_safiq@nstu.edu.bd

Noakhali Science and Technology University

Research Article

Keywords: Breast cancer, Molecular docking, Erα, Tamoxifen, Toxicological effects

Posted Date: August 3rd, 2026

DOI: https://doi.org/10.21203/rs.3.rs-10473636/v1

Additional Declarations: No competing interests reported.

Abstract

Breast cancer in women tends to be the most common cause of cancer-related death, and the causes and progress of the illness are significantly influenced by estrogen receptor alpha (ERα). The current study intended to develop a viable therapeutic candidate from the South Asian plant *Glycine max*, demonstrating efficacy against the ERα in breast cancer through an *in-silico* computational approach. The 3D structures of 84 *Glycine max* proteins were retrieved from the IMPPAT and PubChem databases, respectively. These structures were analyzed and screened by utilizing computational approaches for molecular docking, drug-likeness, pharmacokinetic characteristics, and toxicity prediction. Considering the molecular docking, pharmacokinetic (ADME) properties, drug-likeness, and toxicological effects, two compounds- Beta-Amyrin (-10.3 kcal/mol) and Pseudotaraxasterol (-10.3 kcal/mol) - were selected as the potential inhibitors against the Erα protein. We conducted 100 ns molecular dynamics simulations, Molecular Mechanics Poisson-Boltzmann Surface Area (MM/PBSA), and Principal Component Analysis (PCA) to analyze the stability and interactions of the compounds as protein-ligand complexes, using Tamoxifen as a control drug. Overall, the findings of this study strongly suggest that the selected compounds have the potential to act as inhibitors against the ERαprotein of breast cancer, offering promising prospects for the treatment and management of breast cancer.

Introduction

Breast cancer is a prevalent and complex disease originating from breast tissue cells, impacting millions of people worldwide, primarily women (Akram et al., 2017). Breast cancer is among the most common malignancies globally, with approximately 2.3 million new cases diagnosed annually, representing around 25% of all cancers in women (McPherson et al., 1994; Sung et al., 2021). In Bangladesh, the incidence rate is around 22.5 cases per 100,000 females, and it ups 19.3 per 100,000 in women aged between 15 and 44 years (Sultana et al., 2022). The most common symptom of breast cancer is a painless lump in the breast, which often goes undiagnosed in its early stages (Coleman, 2017). This malignity originally arises from the ducts or lobules of the breast and, via metastasis, spreads to other sites of the body through either lymphatic or blood systems (Bisoyi, 2022). Regular self-examinations, clinical screenings, and mammograms are crucial in early detection (Coleman, 2017). Breast cancer responds better to therapy when detected early, increasing survival rates and lowering morbidity (Coleman, 2017). Patient outcomes have been further improved by innovations in medical interventions, such as tailored therapy regimens and targeted medications (Coleman, 2017). In order to combat the disease and reduce its death rate, it is imperative to raise awareness and guarantee easy access to medical care (Coleman, 2017). The primary molecular targets in breast cancer are estrogen receptor alpha (ERα) and progesterone receptor; both appear in around 70% of total breast cancer cases (Ellmann et al., 2009; Saha et al., 2019). Besides, another imperative marker used for breast cancer subtyping is the epidermal growth factor receptor 2 (HER2), which is overexpressed in approximately 20% of all cases (Parise et al., 2009). The molecular nature of breast cancer is also influenced by several risk factors, such as age, sex, genetic predisposition, family history, and a sedentary lifestyle, understanding these risk factors is critical as they assist early diagnosis, high-risk individuals and guide preventive measures (Rohel et al., 2023).

Estrogen, a vital sex hormone, is synthesized in the forms of oestrone (E1), oestradiol (E2), and oestriol (E3), with oestradiol being the most potent and dominant in premenopausal women, and its role in breast cancer

is closely tied to its interaction with estrogen receptors, particularly ERα playing critical role in female development and maintenance (Nlsson and Gustafsson, 2002; Humphries et al., 2002; Bartkowiak et al., 2024). The ERα receptor regulates cell proliferation and survival by dimerizing and activating gene transcription in response to oestrogen (Pinzone et al., 2004). When complexed with estrogen, the ERα receptor dimerizes to regulate gene transcription, influencing cell proliferation and survival; ER positive breast cancers are typically responsive to endocrine therapies like Tamoxifen, aromatase inhibitors, and selective oestrogen receptor downregulators, but resistance develops over time, complicating long-term management and necessitating novel treatment approaches (Raheem et al., 2023; Howell et al., 2004; Jordan, 2015; Grober et al., 2011).

The discovery of novel chemicals, particularly from nature, has become a critical source in cancer treatment by blending traditional plant-based medicine with modern molecular approaches to adopt their high structural diversity and wide spectrum of bioactivity (Gordaliza; 2007). Soybean (*Glycine max*), a globally traded legume, belonging the family of Fabaceae and its seeds are rich in bioactive isoflavones (phytoestrogens) such as genistein, daidzein, and glycitein, which can mimic estrogen and interact with ERα, potentially modulating its transcription activity, makes soybean a promising candidate against breast cancer treatment (Abdulkadir et al., 2024; Fuentes and Silveyra, 2019; Das et al., 2020).

Computational methods, especially molecular docking enables virtual screening of compound libraries to find potential active molecules (Pinzi and Rastelli, 2019). During this current investigation, we screened 84 compounds for their capacity to bind ERα using molecular docking, followed by 100 ns molecular dynamics simulations to assess stability. Further *in silico* analysis investigated pharmacokinetics, toxicity, and biological activity of selected phytoestrogen to establish the therapeutic potentials to aid the development of safer and effective breast cancer treatments.

Materials and Methods

Protein preparation

The protein structure of human ERα complexed with 4-hydroxytamoxifen (PDB code: 3ERT, R-Value Free: 0.262, R-Value Work: 0.229) at a resolution of 1.9 Å was obtained from the Protein Data Bank in PDB format (Rose et al., 2017). The PDB is a repository of data regarding experimental protein and nucleic acid structures (Rose et al., 2017). This PDB ID was selected due to its origin (*Homo sapiens*) and superior resolution compared to other PDB structure IDs (Rose et al., 2017). Protein chain (A) in Fig. 1 has 261 amino acid residues and possesses a molecular weight of 30.24 kDa. To prepare for molecular docking and dynamic simulation, BIOVIA Discovery Studio software was utilized to exclude water molecules, heteroatoms, and inhibitor molecules, while also including polar hydrogen atoms (Ayodele et al., 2023; Dassault Systemes, 2024). BIOVIA Discovery Studio Visualiser is a complimentary, comprehensive molecular modelling program designed for the visualization, sharing, and analysis of protein and small molecule data (Verma et al., 2022).

Ligand preparation

A total of 84 notable phytoconstituents from the medicinal plant *Glycine max* were extracted from the Indian Medicinal Plants, Phytochemistry, and Therapeutics database, IMPPAT 2.0 (Vivek-Ananth et al., 2023). The three-dimensional structures of phytocompounds were acquired from PubChem in SDF format (Kim et al., 2016). PubChem provides data on chemical compounds, including their structure, molecular formula, molecular weight, and more. Subsequently, the compounds were transformed into PDB format via Open Babel software and their energy was minimized to guarantee compatibility with molecular docking experiments (O' Boyle et, 2011). The 3D structure of the standard control chemical (Tamoxifen, CID ID: 2733526) was obtained in SDF format for further comparison with the phytocompounds (Roy et al., 2021).

Virtual screening and molecular docking

Molecular docking analysis was employed to examine binding affinity and interaction types, while molecular screening was utilized to identify lead compounds with desirable biological functions. PyRx is an open-access virtual screening tool designed for evaluating extensive libraries of chemicals against specific therapeutic targets (Hempel et al., 2015). AutoDock4 and AutoDock Vina are the two most efficient tools inside PyRx that provide an intuitive interface for conducting molecular docking in computer-aided drug creation (Dallakyan, 2015). We used PyRx V.0.8 GUI and AutoDock Vina for the molecular docking of the chosen phytocompounds and the target protein of our study. The target protein was prepared and converted into a macromolecule for docking purposes. Thereafter, Open Babel is employed to import and prepare the ligands within the software (Saxena and Mishra, 2023). The ligands were minimized using the default settings, incorporating hydrogen and Gasteiger charges, and translated to pdbqt format (Saxena and Mishra, 2023). The grid box parameters were established at X = 22.5188, Y = 5.4029, Z = 21.8576, and executed with an exhaustiveness of 8. The ligands were selected based on their maximum binding affinity. The rest compounds were rejected due to a binding affinity of ≤ 9.0 kcal/mol. The Discovery Studio 2024 program was utilized to visualize protein-ligand interactions, enabling a comprehensive analysis of the particular bonds and amino acid residues present in the binding areas (Dassault Systemes, 2024).

Forecasting drug-likeness and ADME characteristics

SwissADME is a web-based computational tool utilized to illustrate the ADME characteristics of chosen phytochemicals (Daina et al., 2017). The essential characteristics linked to ADME properties, including Lipinski's rule of five, were presented. The Simplified Molecular Input Line Entry System (SMILES) was employed to generate the list, featuring one input molecule per line with numerous entries. The results are presented for each molecule in tables, graphs, and an Excel spreadsheet. Our current research seeks to assess the correlation between the drug-like characteristics of candidate compounds and their oral bioavailability, utilizing the Lipinski rule. The Lipinski rule of five posits that the probability of inadequate absorption or permeation escalates when the number of hydrogen bond donors (HBD) is ≥ 5, the number of hydrogen bond acceptors (HBA) is ≥ 10, the molecular weight (MW) is ≥ 500, and the calculated Log P (iLogP) surpasses 5 (or MlogP > 4.15) (Lipinski, 2017). Before categorizing a molecule as a drug, its pharmacokinetic (PK) properties, including absorption, distribution, metabolism, and excretion (ADME), physicochemical characteristics, blood-brain barrier permeability, hydrophobicity, and lipophilicity are thoroughly evaluated through computer-based analysis (Hou and Xu, 2003).

Forecasting toxicological characteristics

It is essential to assess the toxicological properties of drug candidates and confirm their safety prior to granting approval for any new medication. The ProTox-III online web server was utilized to evaluate the toxicological characteristics of the selected compounds (Banerjee et al., 2018). This platform provides predictions for the values of oral toxicity, hepatotoxicity, cytotoxicity, carcinogenicity, immunotoxicity, and mutagenicity.

Molecular dynamics simulation

Molecular dynamics simulation elucidated the physical movements of the atoms and molecules inside the bound protein-ligand complex (Michaud-Agarwal et al., 2011). We utilized the YASARA Dynamics tool to examine the dynamic behavior of the ligand-3ERT complex over several time scales to assess the binding stability of the ligands to the 3ERT protein (Land and Humble, 2018). The two optimal complexes (3ERT-CID73145, 3ERT-CID12305110) and the control (3ERT-CID2733526) were chosen for the molecular dynamic simulation, which lasted 100 ns with intervals of 0.25 ns each (Land and Humble, 2018).

During the preliminary stage of the simulation, the 3ERT-drug complex underwent a purification step to enhance its structure, including the hydrogen bond network. The grid size of (96.9654 x 96.9654 x 96.9654) Å were later determined to create a cubic box with periodic cell boundary conditions. We employed the AMBER14 force field within a cubic box to conduct simulations of the ligand-3ERT complex in a simulated aqueous environment (Wallace et al., 1995). We introduced supplementary sodium (Na^+) and chlorine (Cl^-) ions into the cubic box via the TIP3P approach to attain system neutrality. Subsequently, we employed the steepest descent approach to minimize the energy of the drug-3ERT combination. Conversely, we employed the Particle Mesh Ewald (PME) computation method to assess the long-range Coulomb interactions (Roy et al., 2021). This research was performed under physiological circumstances at a temperature of 298 K, a pH of 7.4, and a sodium chloride concentration of 0.9% (Roy et al., 2021). The trajectory data were evaluated at the conclusion of the 100 ns simulation to compute the RMSD (root mean square deviation), RMSF (root mean square fluctuation), Rg (radius of gyration), and SASA (solvent accessible surface area) values (Salentin et al., 2015).

MM-PBSA analysis/energy of binding analysis method

Molecular Mechanics Poisson-Boltzmann Surface Area (MMPBSA) methods are employed to determine the binding affinity of protein-ligand interactions, given their remarkable connection with results from experiments and efficiency (Kumari et al., 2014). In the context of rescoring ligand-protein complexes predicted by docking, binding free energy assessment approaches can serve as a valuable and effective tool, providing more precise estimates of ligand-protein binding affinities than simple scoring functions. Different ligand orientations generated by docking software are utilized as starting ligand-receptor coordinates for molecular dynamics simulations to accomplish this objective. The MD simulations undergo additional processing through the MPBSA evaluation. The most reliable ligand orientation is determined by comparing the optimal binding free energy obtained (Honig and Nicholls, 1995; Cheng et al., 2012). The stable region of

the three compounds with ER alpha complexes was employed to produce a 100 ns molecular dynamics trajectory for MM-PBSA computations.

The binding energy components were measured using the MMPBSA technique in the YASARA simulator (YASARA Biosciences). The g_mmpbsa tool calculates the protein-ligand complex's binding energy using the following equation.

$\Delta G_{Binding} = G_{Complex} - (G_{Protein} + G_{Ligand})$

Where $G_{Complex}$ denotes the binding complex's total free energy, and $G_{Protein}$ and G_{Ligand} denote the total free energies of the three molecules bound to ER-alpha, respectively.

Results

Molecular docking and interpretation of ligand protein interaction

The docking study utilized the crystal structure of human estrogen receptor alpha (ER-α). We employed the Indian Medicinal Plants, Phytochemistry and Therapeutics (IMPPAT) Library for the purpose of docking. The 84 phytoconstituents of *Glycine max* plant exhibit binding affinities ranging from − 3.9 to -10.3 kcal/mol, while six of them exhibit binding affinities ranging from − 9.6 to -10.3 kcal/mol, as presented in **Supplementary Table 1** as well as these compounds were selected for further evaluation. In this study, the control ligand was tamoxifen (CID ID: 2733526) which exhibited a binding affinity of -6.8 kcal/mol. The two selected compounds (Beta-Amyrin: CID73145, Pseudotaraxasterol: CID12305110) with the highest binding affinity, along with the structural analysis of control (Tamoxifen: CID 2733526) are presented in Fig. 1 **and** Table 1. The investigation suggested that Beta-Amyrin it exhibited one Pi-Sigma (π-σ) bond at the TRP383 (3.56 Å) position as well as there were seven alkyl bonds at LEU525 (5.22 Å), LEU536 (4.57 Å), LEU536 (5.23 Å), LEU536 (4.06 Å), LEU354 (3.91 Å), LEU536 (4.54 Å), and LEU354 (4.91 Å), respectively. There were also eight π-alkyl bonds at TRP383 (5.11 Å), TRP383 (5.45 Å), TRP383 (4.2 Å), TRP383 (5.19 Å), TRP383 (5.1 Å), TRP383 (4.26 Å), TYR526 (4.99 Å), and TYR526 (4.72 Å), respectively. The compound Pseudotaraxasterol showed two π-σbonds at TRP383 (3.93 Å), and TRP383 (3.35 Å) as well as there were five π-alkyl bonds at TRP383 (5.35 Å), TRP383 (5.42 Å), TRP383 (4.15 Å), TRP383 (4.95 Å), and TYR526 (4.74 Å). And there were many alkyl bonds presented in following distance: ALA350 (4.25 Å), ALA350 (4.18 Å), LEU525 (4.69 Å), LYS529 (5.13 Å), LEU536 (4.8 Å), LEU525 (4.81 Å), LYS529 (3.9 Å), LYS529 (4.32 Å), VAL533 (5.25 Å), LEU354 (4.85 Å), LEU536 (3.91 Å), LEU354 (3.89 Å). Lastly, the control (tamoxifen) showed nine bonds in total, one π-σ at ILE424 (3.96 Å), one alkyl bond at MET421 (4.88 Å), and others are π-alkyl bonds at PHE404 (5.47 Å), ALA350 (3.97 Å), LEU525 (4.97 Å), LEU346 (4.97 Å), LEU387 (5.13 Å), MET421 (5.13 Å), and at LEU525 (5.06 Å). From this ligand-protein interaction we observed that, pseudotaraxasterol (CID 12305110) showed two alkyl bonds ALA350 residue of the protein at 4.25 Å, 4.18 Å distance while the control Tamoxifen (CID 2733526) showed only one π-alkyl bond at 3.97 Å. Moreover, at the LEU525 residue, Beta-Amyrin (CID 73145) showed one alkyl bond, pseudotaraxasterol showed two alkyl bond, and the control exhibited two π-alkyl bonds at 5.22 Å, 4.69 Å, 4.81 Å, 4.97 Å, and 5.06 Å respectively. The residues of non-bond interactions and bond categories are given in **Supplementary Table 2**.

Examination of Drug-Like characteristics and ADME evaluation

The pharmacokinetic properties are essential in the realm of drug development, as they dictate the characteristics of an effective oral medication, including its metabolism and elimination, all while minimizing the risk of adverse effects (Yang et al., 2019). Due to the low pharmacokinetic profiles, numerous pharmaceuticals are unable to progress to market during clinical trials. Table 2 presents the evaluation outcomes concerning the drug-likeliness profile of the chosen substances. In the realm of drug discovery, Lipinski's rule of five functions as a computational framework to evaluate solubility, membrane permeability, and pharmacological effectiveness (Bahugina et al., 2017). The determination is contingent upon four critical factors: molecular weight, the quantity of hydrogen bond donors, the quantity of hydrogen bond acceptors, and the logarithmic value of the partition coefficient. Our investigation demonstrates that the two chosen phytocompounds, “CID 12305110” and “CID 73145,” adhere to the Lipinski criteria, exhibiting only one violation and possessing a molecular weight of under 500. Furthermore, they exhibit fewer than 10 hydrogen bond acceptors, with hydrogen bond donors being less than 5, and an octanol-water partition coefficient (iLOGP) of less than 5. In addition to adhering to the Lipinski rules, these two compounds also conform to the supplementary four criteria established by Hopkins. Specifically, both compounds exhibit a topological polar surface area (TPSA) ranging from 20 to 21 A2, possess 31 heavy atoms, contain no rotatable bond, and are devoid of any undesirable structural alerts, as illustrated in Table 2.

Table 2
List of pharmacokinetic properties includes physicochemical properties, lipophilicity, water solubility, drug-likeness and medicinal chemistry of four selected compounds (Yang et al., 2019; Bahugina et al., 2017; Roehm et al., 1991).

Properties	Attributes	Pubchem ID: 73145	Pubchem ID: 12305110
Physiochemical Properties	MW(g/mol)	426.72 g/mol	426.72 g/mol
	Heavy atoms	31	31
	Arom.heavy atoms	0	0
	Rotable bonds	0	0
	H-bond acceptor	1	1
	H-bond donor	1	1
	TPSA	20.23 A2	20.23 A2
Lipophilicity	Log P (o/w)	4.74	4.77
Water Solubility	Log S (ESOL)	-8.25	-8.09
Pharmacokinetics	GI absorption	Low	Low
	BBB permeant	No	No
Drug-likeliness	Lipinski	Yes	Yes
	Bioavailability score	0.55	0.55
Medicinal Chemistry	Synthetic accessibility	6.04	6.17

Furthermore, these compounds demonstrated a bioavailability score of 0.55. Figure 2 shows the top two compounds exhibit the following parameters: POLAR (Polarity), INSOLU (Insolubility), INSATU (Instauration), FLEX (Rotable bond flexibility), LIPO (Lipophilicity), SIZE (Molecular Weight), and nearly entirely fall into the colored zone that denotes an appropriate physio-chemical space for oral bioavailability. Ultimately, this analysis reveals that the natural compounds “CID 12305110” and “CID 73145” meet all the fundamental criteria for classification as drug-like compounds. Additionally, both molecules satisfy the requirements for an ideal LogP (octanol/water). All of them fall between 0 and 5, which is the ideal range (Roehm et al., 1991). Nevertheless, neither of these drugs penetrates the blood-brain barrier (BBB) effectively, and both have low GI absorption value.

Predictions of toxicity

Currently, toxicity prediction is an essential phase in medication design to assess the adverse effects of a certain molecule on humans, plants, and the environment. Traditional methods include several animal experiments to evaluate the toxicity of chemicals, which are not only expensive and time-consuming but also raise significant ethical issue (Muhammad et al., 2018). Computer-aided toxicity prediction is more efficient and cost-effective, yielding findings more often. This diminishes the quantity of biological experimental assessments. The ProTox-III server was utilized to forecast the toxicological features of the two chemicals,

as seen in Table 3. The results suggest that none of the substances are likely to exhibit neurotoxicity, hepatotoxicity, mutagenicity, or cytotoxicity, but may demonstrate immunotoxicity.

Concerning acute oral toxicity, the CID 73145 chemical exhibited modest toxicity (Hodge and Sterner, 2005), with an LD50 value of 1190 mg/kg, categorizing it in class IV of the Global Harmonised System (GHS), which suggests it may be detrimental if ingested. Compound CID 12305110 had an LD50 value of 70,000 mg/kg. According to Hodge and Sterner (2005), it is classified as class VI (LD50 > 5000), indicating it is non-toxic (Guo et al., 2021).

Table 3
Toxicity profiling of top two compounds through ProTox-III Online server.

Compound (Pubchem ID)	Hepatotoxicity	Carcinogenicity	Mutagenicity	Cytotoxicity	LD_{50} Value(mg/kg)	Predicted Toxicity Class
CID 73145	Inactive	Inactive	Inactive	Inactive	1190	IV
CID 12305110	Inactive	Inactive	Inactive	Inactive	70000	VI
CID 2733526	Active	Inactive	Inactive	Inactive	1190	IV

Molecular Dynamic Simulation

In the current study, 100 ns MD simulations of the most potent inhibitors was conducted in relation to the target, which is the "human estrogen receptor alpha ligand-binding domain" (PDB ID: 3ERT). This was important because docking studies only show one scene while biomolecules behave dynamically. In comparison to the control, all the compounds exhibited a consistent dynamic configuration of ER alpha.

Root means square deviation (RMSD)

Root Mean Square Deviation (RMSD) is often used to evaluate the stability of the receptor-ligand complex in molecular dynamics simulation. Overall, having a mean RMSD of 2.243 Å, CID 73145 complex reported stable, though there are some peaks observed in its RMSD plot (Fig. 3). The complex revealed stability during the first 64 ns, after that minor deviations were observed at 74.25 and 79.25 ns which were 2.856 Å and 2.841 Å, respectively, as well as there is a maximum peak of 2.996 Å at 74.5 ns (Fig. 3). The mean RMSD of CID 1235110 complex is 2.353 Å which also revealed stable behaviour. Though there are some major peaks observed in the RMSD plot during 29 ns to 35.75 ns and at 44.25 ns as well as the maximum peak was of 3.228 Å at 32.75 ns (Fig. 3). On the other hand, the CID 2733526 (control) complex maintained a distorted high RMSD value for a long period. Mean RMSD of this complex was 2.769 Å and RMSD value was always higher than 3 Å during 22 to 93.5 ns. Comparatively, the CID 73145 complex showed a better result of root mean square deviation (RMSD) than the others.

Root means square fluctuation (RMSF)

To evaluate the structural dynamics of the protein residues, the RMSF values were computed. These values reveal the flexibility of the protein residues in reaction to the ligand binding during the simulation. The CID 73145 complex have a highest RMSF peak of 7.35 Å at ALA 551 and a second highest RMSF peak of 7.13 at ARG 548. From the RMSF plot, there is a highest peak of 9.86 Å and a second highest peak of 8.05 Å of the CID complex whereas CID 2733526 (control) complex have a highest peak of 8.87 Å and a second highest peak of 7.72 Å at ALA 551 and HIS 550 residues, respectively (Fig. 4). The mean root mean square fluctuation (RMSF) values of CID 73145, CID 12305110, and CID 2733526 (control) are 1.505 Å, 1.617 Å, and 1.686 Å, respectively (Fig. 4). This result suggests that compared to control, CID 73145 induced minimal conformational change of protein and CID 12305110 induced some major active site conformational shifts.

Radiation of gyration (Rg)

Protein's compactness and folding behavior can be understood through analyzing the overall conformational state and its relation to the tertiary structure, which is known as the radius of gyration (Rg). The radius of gyration (Rg), as a function of time, was used to evaluate the structural compactness. The average Rg values were 19.010 Å, 19.081 Å, and 18.990 Å as observed for CID 73145, CID 12305110, and CID 2733526, respectively (Fig. 5). For CID 73145, the Rg values range from 18.80 Å to 19.20 Å for ~ 90%-time period of the simulation. In case of CID 12305110, ~ 95%-time period maintained a Rg fluctuation from to 18.89 Å to 19.27 Å. Moreover, CID 2733526 (control) complex maintain a Rg fluctuation of 18.80 Å to 19.18 Å only for ~ 70%-time period (Fig. 5). These fluctuations indicate that the active site of the protein is less likely undergo significant conformational changes when binding with CID 73145 and CID 12305110 except CID 2733526.

Solvent-accessible surface area (SASA)

The solvent-accessible surface area (SASA) indicates the portion of a biomolecule's surface that is available to solvent molecules. This measurement is essential for understanding the free energy associated with protein-ligand binding, protein folding, and interactions between proteins. CID 73145, CID 12305110, and CID 2733526 (control) have an average SASA value of 12996.738, 12956.616, and 12790.524, respectively (Fig. 6). There is no significant inconsistency of the SASA values of these complexes.

Hydrogen bond interactions

The mean number of hydrogen bonds between solute and solvent for CID 73145, CID 12305110, and CID 2733526 are 405.180, 404.476, and 399.504, respectively (Fig. 7). There is no significant difference of hydrogen bonds number between these complexes.

Molecular mechanics Poisson Boltzmann surface area (MM/PBSA)

The average binding energy for CID 73145, CID 12305110, and CID 2733526 (control) are 103.348 kJ/mol, 115.638 kJ/mol, and 20.247 kJ/mol (Fig. 8). Though control has a lower binding energy compared to other complexes, several large fluctuations in the MM/PBSA graph indicates that protein's active side residues might alter and as a result there might be an unstable complex formation due to these fluctuations. On the

other hand, CID 73145 and CID 12305110 have moderate binding with the protein complex as there are consistent binding energies ranges from 50 kJ/mol to 150 kJ/mol.

Discussion

In contemporary contexts, CADD has become an essential instrument in the realm of drug development methodologies, significantly reducing costs, time, and labour involvement (51). CADD constrains the biological research undertaken by scientists and simultaneously alleviates ethical concerns, thereby accelerating the drug innovation process (Li et al., 2013). Molecular docking, ADMET, and MD simulation represent the methodologies of CADD that demonstrate commendable biological efficacy (Hopkins, 2007). Through a series of studies, we discovered that molecular docking effectively predicts the binding modes of protein-ligand interactions, while MD simulation elucidates the complex interactions between the two, thereby ranking small compounds as promising candidates for specific drug efficacy (Chandran and Patwardhan, 2017; Janaki et al., 2021; Xu et al., 2021; Verma et al., 2022). This study involved a comprehensive analysis and screening of 84 compounds aimed at targeting the ERα protein for the treatment of neurological disorders. Molecular docking was performed to evaluate if the compounds exhibiting greater binding affinity (Janaki et al., 2021; Yang et al., 2017). In our investigation, the foremost two compounds were identified due to their superior binding capacity with the ligand, specifically PubChem CID 73145 and PubChem CID 12305110, both exhibiting a binding score of -10.3 kcal/mol. Diverse forms of interactions at a distance typically confirm the significance of protein-ligand interactions, which are crucial for forecasting the binding affinities between ligands and proteins. All molecules demonstrated a range of unbound and bound interactions with numerous residues at the site or its periphery. In the ERα protein, control (CID 2733526) exhibited nine hydrophobic interactions with the residues ILE A: 424, MET A: 421, PHE A: 404, ALA A: 350, LEU A: 346, LEU A: 387, and LEU A: 525 (π-σ, alkyl, and π-alkyl). “CID 73145” exhibited sixteen hydrophobic interactions (alkyl, π--alkyl, and π-σ) with TRP A: 383, LEU A: 525, LEU A: 536, LEU A: 354, and TYR A: 526. “CID 12305110” exhibited a total of twenty hydrophobic interactions, including π-σ, π-alkyl, and alkyl types, with the following residues: TRP A: 383, ALA A: 350, LEU A: 525, LYS A: 529, LEU A: 536, VAL A: 533, LEU A: 354, LEU A: 354, and TYR A: 526. The diverse forms of hydrophobic interactions, including π-σ, π-alkyl, and alkyl, between the ERα protein and various compounds with distinct protein residues are illustrated in **Supplementary Table 2** and Fig. 1.

Subsequently, we assessed the pharmacokinetic properties, as the optimization of these characteristics is essential for compounds to successfully navigate standard clinical trials and emerge as viable drug candidates (Yang et al., 2017). The molecular weight and polar surface topological area (TPSA) values exhibit an inverse relationship with molecular permeability; higher values correspond to diminished permeability, while lower values are indicative of enhanced permeability (Prasanna and Doerksen, 2008; Rawat et al., 2024). LogP serves as a measure of lipophilicity, defined as the logarithm of the partitioning between inorganic and aqueous phases (Tshepelevitsh et al., 2020). Lipophilicity determines a drug's absorption capacity; lower LogP values often indicate better absorption (Box and Comer, 2008). Another important factor is solubility, which is determined by LogS; lower values are advantageous for effective therapeutics solubility (Saxena and Mishra, 2023; Box and Comer, 2008). When the quantity of hydrogen bond acceptors and donors surpasses the optimal range, it negatively impacts the ability of drug molecules to traverse the

membrane bilayer (Coimbra et al., 2020). The quantity of rotatable bonds ought to remain below 10, as exceeding this threshold could potentially influence oral bioavailability (Veber et al., 2002). Our assessment of ADMET properties for the docked compounds indicates that both compounds fall within the acceptable range for consideration as potential drug candidates. Given that our pharmaceutical agent must exert its effects on neurological conditions, it is imperative that it successfully traverses the blood-brain barrier, a fundamental criterion in the realm of drug discovery (Curtaz et al., 2022). A harmful substance possesses the capability to inflict harm on a living organism (Roy et al., 2021). Research indicates that toxicity plays a significant role in the failures observed during the later stages of drug development. The efficacy of *in silico* toxicity analysis is notable, as it addresses the limitations inherent in traditional methodologies, such as the necessity for animal testing, exorbitant costs, and the considerable time investment required by in vivo techniques. An analysis of the toxicity profile of the two leading compounds has been conducted using *in silico* methods. The information derived from the toxicity examination server indicates that none of the compounds exhibit carcinogenic or mutagenic properties. The LD50 primarily offered insights into the immediate or acute toxicity of compounds, revealing their optimal characteristics within the study.

As MD simulation evaluates the actual dynamics of atoms, it has become an essential tool for CADD (Hernández-Rodríguez et al., 2016). In this study, MD simulation was investigated for two lead compounds along with a control. From the dynamic simulation result, the RMSD, RMSF, SASA, MM-PBSA, H-bond formation, and the radiation of gyration were reported. The investigation revealed that compared to the control (CID 2733526), CID 73145 had the lowest mean RMSD (2.243 Å) and no unusual changes in the RMSF plot, suggesting that this complex maintained a stable binding. Although the Rg values for the three complexes were quite similar (19.010 Å, 19.081 Å, and 18.990 Å), CID 73145 and CID 12305110 showed fewer fluctuations over time, but CID 2733526 (the control) deviated from its mean Rg values most of the time. None of these complexes showed significant variation in their H-bond formation profiles or SASA value profiles. The MM-PBSA profile indicated that the lead compounds had a greater average binding energies (CID 73145: 103.348 kJ/mol, CID 12305110: 115.638 kJ/mol) compared to the control (CID 2733526: 20.247 kJ/mol). However, there were noticeable fluctuations in the control's MM-PBSA profile compared to the lead compounds, which may suggest that the control showed a potential change in active site conformation. Based on these investigations, it seems that CID 73145, in contrast to the control molecule, established an effective, strong, and robust binding with the target ER_{α} protein. Nevertheless, extensive *in vitro* and *in vivo* studies are necessary for the extracted candidates to enter into the clinical trials and be approved for mankind.

Conclusion

The emergence of breast cancer poses major global health challenges. The current study intended to support breast cancer treatment by using synthetic compounds in the development of new candidates. Since ERα plays a key role in promoting cancer growth, proliferation, and migration, it is considered a potential target for drug development against breast cancer. To address this, we employed various computational techniques to identify new/novel inhibitors of the ERα protein in breast cancer treatment. A dataset of 84 natural compounds was analyzed to evaluate their inhibitory potential. Through virtual screening and molecular docking, two promising lead compounds: Beta-Amyrin and Pseudotaraxasterol, were identified. These

compounds demonstrated strong binding affinities to the ERα protein when compared to the standard drug, Tamoxifen. Further validation through molecular dynamics simulations confirmed the stability of these drug-protein interactions. Additionally, ADMET analysis indicated that the selected compounds have favorable absorption, distribution, metabolism, and excretion profiles, with no probable toxicity concerns. Since this study is entirely based on computational methods, experimental studies will be warranted to confirm the effectiveness of these compounds against in vitro and *in vivo* breast cancer models. The findings of this study are expected to benefit future research in identifying specific pharmacological targets for the development of effective breast cancer therapies.

Declarations

Conflict of interest

Authors declare no known competing financial interests.

Author Contribution

Conceptualization and literature search were performed by GGM, MMEE, MJR and MAH under the supervision of MSH1 and MSI. The first draft of the manuscript was prepared by GGM and MMEE. KF, AH, MSH7, NS, MSH1 and MSI critically analyzed, reviewed and gave suggestions to finalize the manuscript. All authors read and approved the final manuscript.

Acknowledgement

We are thankful to the Dawn of Bioinformatics Ltd, Dhaka, Bangladesh for the valuable suggestion and support.

References

1. Abdulkadir WS, Puana F, Taupik M, Tungadi R, Hutuba AH, Djuwarno EN et al (2024) In Silico Analysis of Isoflavone Compounds in Soybean (Glycine max L) as Anti-Breast Cancer Agents Targeting Estrogen Receptor Alpha. Trop J Phytochem Pharm Sci 3(7):375–379
2. Akram M, Iqbal M, Daniyal M, Khan AU (2017) Awareness and current knowledge of breast cancer. Biol Res 50(1):33
3. Ayodele PF, Bamigbade A, Bamigbade OO, Adeniyi IA, Tachin ES, Seweje AJ et al (2023) Illustrated Procedure to Perform Molecular Docking Using PyRx and Biovia Discovery Studio Visualizer: A Case Study of 10kt With Atropine. Prog Drug Discov Biomed Sci 6(1):a0000424
4. Bahuguna A, Khan I, Bajpai VK, Kang SC (2017) MTT assay to evaluate the cytotoxic potential of a drug. Bangladesh J Pharmacol 12(2):115–118

5. Banerjee P, Eckert AO, Schrey AK, Preissner R (2018) ProTox-II: a webserver for the prediction of toxicity of chemicals. Nucleic Acids Res 46(W1):W257–W263
6. Bartkowiak-Wieczorek J, Jaros A, Gajdzińska A, Wojtyła-Buciora P, Szymański I, Szymaniak J et al (2024) The Dual Faces of Oestrogen: The Impact of Exogenous Oestrogen on the Physiological and Pathophysiological Functions of Tissues and Organs. Int J Mol Sci 25(15):8167
7. Bisoyi P (2022) Malignant tumors – as cancer. In: Understanding Cancer: From Basics to Therapy. Understanding Cancer. pp. 21–36
8. Box KJ, Comer JEA (2008) Using Measured pKa, LogP and Solubility to Investigate Supersaturation and Predict BCS Class. Curr Drug Metab 9(9):869–878
9. Chandran U, Patwardhan B (2017) Network ethnopharmacological evaluation of the immunomodulatory activity of Withania somnifera. J Ethnopharmacol 197:250–256
10. Cheng F, Li W, Zhou Y, Shen J, Wu Z, Liu G et al (2012) admetSAR: a comprehensive source and free tool for assessment of chemical ADMET properties. J Chem Inf Model 52(11):3099–3105
11. Coimbra JTS, Feghali R, Ribeiro RP, Ramos MJ, Fernandes PA (2020) The importance of intramolecular hydrogen bonds on the translocation of the small drug piracetam through a lipid bilayer. RSC Adv 11(2):899–908
12. Coleman C (2017) Early detection and screening for breast cancer. Semin Oncol Nurs 33(2):141–155
13. Curtaz CJ, Kiesel L, Meybohm P, Wöckel A, Burek M (2022) Anti-Hormonal Therapy in Breast Cancer and Its Effect on the Blood-Brain Barrier. Cancers (Basel) 14(20):5132
14. Daina A, Michielin O, Zoete V (2017) SwissADME: a free web tool to evaluate pharmacokinetics, drug-likeness and medicinal chemistry friendliness of small molecules. Sci Rep 7:42717
15. Dallakyan S, Olson AJ (2015) Small-molecule library screening by docking with PyRx. Methods Mol Biol 1263:243–250
16. Das S, Sharangi AB, Egbuna C, Jeevanandam J, Ezzat SM, Adetunji CO et al (2020) Health Benefits of Isoflavones Found Exclusively of Plants of the Fabaceae Family. Functional Foods and Nutraceuticals. Springer, pp 473–508
17. Dassault Systèmes BIOVIA Discovery Studio [Internet]. [cited 2024 Nov 29]. Available from: https://www.3ds.com/products/biovia/discovery-studio
18. Ellmann S, Sticht H, Thiel F, Beckmann MW, Strick R, Strissel PL (2009) Estrogen and progesterone receptors: from molecular structures to clinical targets. Cell Mol Life Sci 66(15):2405–2426
19. Fuentes N, Silveyra P (2019) Estrogen receptor signaling mechanisms. Adv Protein Chem Struct Biol 116:135–170
20. Gordaliza M (2007) Natural products as leads to anticancer drugs. Clin Transl Oncol 9(12):767–776
21. Grober OM, Mutarelli M, Giurato G, Ravo M, Cicatiello L, De Filippo MR et al (2011) Global analysis of estrogen receptor beta binding to breast cancer cell genome reveals an extensive interplay with estrogen receptor alpha for target gene regulation. BMC Genomics 12:36
22. Guo ZH, Li Y, Gong S, Li J, Gong ST, Zhang XS et al (2021) Establishment of 'Network Pharmacology Evaluation Method Guidance'. Chin J Nat Med 19(12):888–896
23. Hempel JE, Williams CH, Hong CC (2015) Chemical Biology: Methods and Protocols. Springer, New York

24. Hernández-Rodríguez M, Rosales-Hernández MC, Mendieta-Wejebe J, Martínez-Archundia M, Correa Basurto J (2016) Current Tools and Methods in Molecular Dynamics (MD) Simulations for Drug Design. Curr Med Chem 23(34):3909–3924
25. Honig B, Nicholls A (1995) Classical electrostatics in biology and chemistry. Science 268(5214):1144–1149
26. Hopkins AL (2007) Network pharmacology. Nat Biotechnol 25(10):1110–1111
27. Hou TJ, Xu XJ (2003) ADME Evaluation in Drug Discovery. 3. Modeling Blood-Brain Barrier Partitioning Using Simple Molecular Descriptors. J Chem Inf Comput Sci 43(6):2137–2152
28. Howell SJ, Johnston SR, Howell A (2004) The use of selective estrogen receptor modulators and selective estrogen receptor down-regulators in breast cancer. Best Pract Res Clin Endocrinol Metab 18(1):47–66
29. Humphries A, Klein D, Baler R, Carter DA (2002) Oestrogen receptors, receptor variants and oestrogen actions in the hypothalamic-pituitary axis. J Neuroendocrinol 14(2):85–94
30. Janaki S, Vijayakumar S, Saran U, Krishnamurthy V, Ramkumar KM (2021) Network pharmacology-based screening of bioactive compounds from Glycyrrhiza glabra against type 2 diabetes. J Biomol Struct Dyn 39(18):6812–6824
31. Jordan VC (2015) The new biology of estrogen-induced apoptosis applied to treat and prevent breast cancer. Endocr Relat Cancer 22(1):R1–31
32. Kim S, Thiessen PA, Bolton EE, Chen J, Fu G, Gindulyte A et al (2016) PubChem Substance and Compound databases. Nucleic Acids Res 44(D1):D1202–D1213
33. Kumari R, Kumar R, Lynn A (2014) g_mx_MM/PBSA—A GROMACS Tool for High-Throughput MM-PBSA Calculations. J Chem Inf Model 54(7):1951–1962
34. Land H, Humble MS (2018) YASARA: A Tool to Obtain Structural Guidance in Biocatalytic Investigations. Methods Mol Biol 1685:43–67
35. Li S, Zhang B (2013) Traditional Chinese medicine network pharmacology: theory, methodology and application. Chin J Nat Med 11(2):110–120
36. Lipinski CA (2016) Rule of five in 2015 and beyond: Target and ligand structural limitations, ligand chemistry structure and drug discovery project decisions. Adv Drug Deliv Rev 101:34–41
37. McPherson KM, Steel CM, Dixon JM (1994) Breast cancer—epidemiology, risk factors, and genetics. BMJ 309(6960):1003–1006
38. Michaud-Agrawal N, Denning EJ, Woolf TB, Beckstein O (2011) MDAnalysis: A toolkit for the analysis of molecular dynamics simulations. J Comput Chem 32(10):2319–2327
39. Muhammad J, Khan A, Ali A, Fang L, Yanjing W, Xu Q et al (2018) Network pharmacology: exploring the resources and methodologies. Curr Top Med Chem 18(12):949–964
40. Nilsson S, Gustafsson JÅ (2002) Biological role of estrogen and estrogen receptors. Crit Rev Biochem Mol Biol 37(1):1–28
41. O'Boyle NM, Banck M, James CA, Morley C, Vandermeersch T, Hutchison GR (2011) Open Babel: An open chemical toolbox. J Cheminform 3:33

42. Parise CA, Bauer KR, Brown MM, Caggiano V (2009) Breast cancer subtypes as defined by ER, PR, and HER2 among women with invasive breast cancer in California, 1999–2004. Breast J 15(6):593–602
43. Pinzi L, Rastelli G (2019) Molecular Docking: Shifting Paradigms in Drug Discovery. Int J Mol Sci 20(18):4331
44. Pinzone JJ, Stevenson H, Strobl JS, Berg PE (2004) Molecular and Cellular Determinants of Estrogen Receptor α Expression. Mol Cell Biol 24(11):4605–4612
45. Prasanna S, Doerksen RJ (2008) Topological Polar Surface Area: A Useful Descriptor in 2D-QSAR. Curr Med Chem 16(1):21–41
46. Raheem F, Karikalan SA, Batalini F, El Masry A, Mina L (2023) Metastatic ER+ Breast Cancer: Mechanisms of Resistance and Future Therapeutic Approaches. Int J Mol Sci 24(22):16198
47. Rawat K, Tewari D, Bisht A, Chandra S, Tiruneh YK, Hassan HM et al (2024) Identification of AChE targeted therapeutic compounds for Alzheimer's disease: an in-silico study with DFT integration. Sci Rep 14(1):30356
48. Roehm NW, Rodgers GH, Hatfield SM, Glasebrook AL (1991) An improved colorimetric assay for cell proliferation and viability utilizing the tetrazolium salt XTT. J Immunol Methods 1991;142(2):257–65
49. Roheel A, Khan A, Anwar F, Akbar Z, Akhtar MF, Khan MI et al (2023) Global epidemiology of breast cancer based on risk factors: a systematic review. Front Oncol 13:1240098
50. Rose PW, Prlić A, Altunkaya A, Bi C, Bradley AR, Christie CH et al (2017) The RCSB protein data bank: integrative view of protein, gene and 3D structural information. Nucleic Acids Res 45(D1):D271–D281
51. Roy AS, Sawrav MSS, Hossain MS, Johura FT, Ahmed SF, Hami I et al (2021) In silico identification of potential inhibitors with higher potency than bumetanide targeting NKCC1: An important ion co-transporter to treat neurological disorders. Inf Med Unlocked 27:100777
52. Saha T, Makar S, Swetha R, Gutti G, Singh SK (2019) Estrogen signaling: an emanating therapeutic target for breast cancer treatment. Eur J Med Chem 177:116–143
53. Salentin S, Schreiber S, Haupt VJ, Adasme MF, Schroeder M (2015) PLIP: fully automated protein–ligand interaction profiler. Nucleic Acids Res 43(W1):W443–W447
54. Saxena R, Mishra S (2023) In silico Screening and Identification of Inhibitor Molecules Targeting SDS22 protein. Orient J Chem 39(3):647–656
55. Sultana R, Khatun N, Islam R, Rahman MFP (2022) Assessment of risk factors for distant metastases of breast cancer. Planet (Barisal) 6(2):408–421
56. Sung H, Ferlay J, Siegel RL, Laversanne M, Soerjomataram I, Jemal A et al (2021) Global cancer statistics 2020: GLOBOCAN estimates of incidence and mortality worldwide for 36 cancers in 185 countries. CA Cancer J Clin 71(3):209–249
57. Tshepelevitsh S, Kadam SA, Darnell A, Bobacka J, Rüütel A, Haljasorg T et al (2020) LogP determination for highly lipophilic hydrogen-bonding anion receptor molecules. Anal Chim Acta 1132:123–133
58. Veber DF, Johnson SR, Cheng HY, Smith BR, Ward KW, Kopple KD (2002) Molecular Properties That Influence the Oral Bioavailability of Drug Candidates. J Med Chem 45(12):2615–2623
59. Verma AK, Ahmed SF, Hossain MS, Bhojiya AA, Mathur A, Upadhyay SK et al (2022) Molecular docking and simulation studies of flavonoid compounds against PBP-2a of methicillin-resistant Staphylococcus

aureus. J Biomol Struct Dyn 40(21):10561–10577

60. Verma AK, Majid A, Hossain MS, Ahmed SF, Ashid M, Bhojiya AA et al (2022) Identification of 1,2,4-Triazine and Its Derivatives Against Lanosterol 14-Demethylase (CYP51) Property of Candida albicans: Influence on the Development of New Antifungal Therapeutic Strategies. Front Med Technol 4:845322
61. Vivek-Ananth RP, Mohanraj K, Sahoo AK, Samal A (2023) IMPPAT 2.0: An Enhanced and Expanded Phytochemical Atlas of Indian Medicinal Plants. ACS Omega 8(9):8827–8845
62. Wallace AC, Laskowski RA, Thornton JM (1995) LIGPLOT: a program to generate schematic diagrams of protein-ligand interactions. Protein Eng 8(2):127–134
63. Xu T, Wu M, Feng J, Lin X, Guo J, Zhao J et al (2021) Network pharmacology-based prediction of active compounds in Triptolide and potential targets for rheumatoid arthritis treatment. Front Pharmacol 12:614995
64. Yang H, Lou C, Sun L, Li J, Cai Y, Wang Z et al (2019) admetSAR 2.0: web-service for prediction and optimization of chemical ADMET properties. Bioinformatics 35(6):1067–1069
65. Yang MM, Wang J, Dong L, Kong DJ, Teng Y, Liu P et al (2017) Lack of association of C3 gene with uveitis: Additional insights into the genetic profile of uveitis regarding complement pathway genes. Sci Rep 7(1):1–8

Table

Table 1 is available in the Supplementary Files section.

Figures

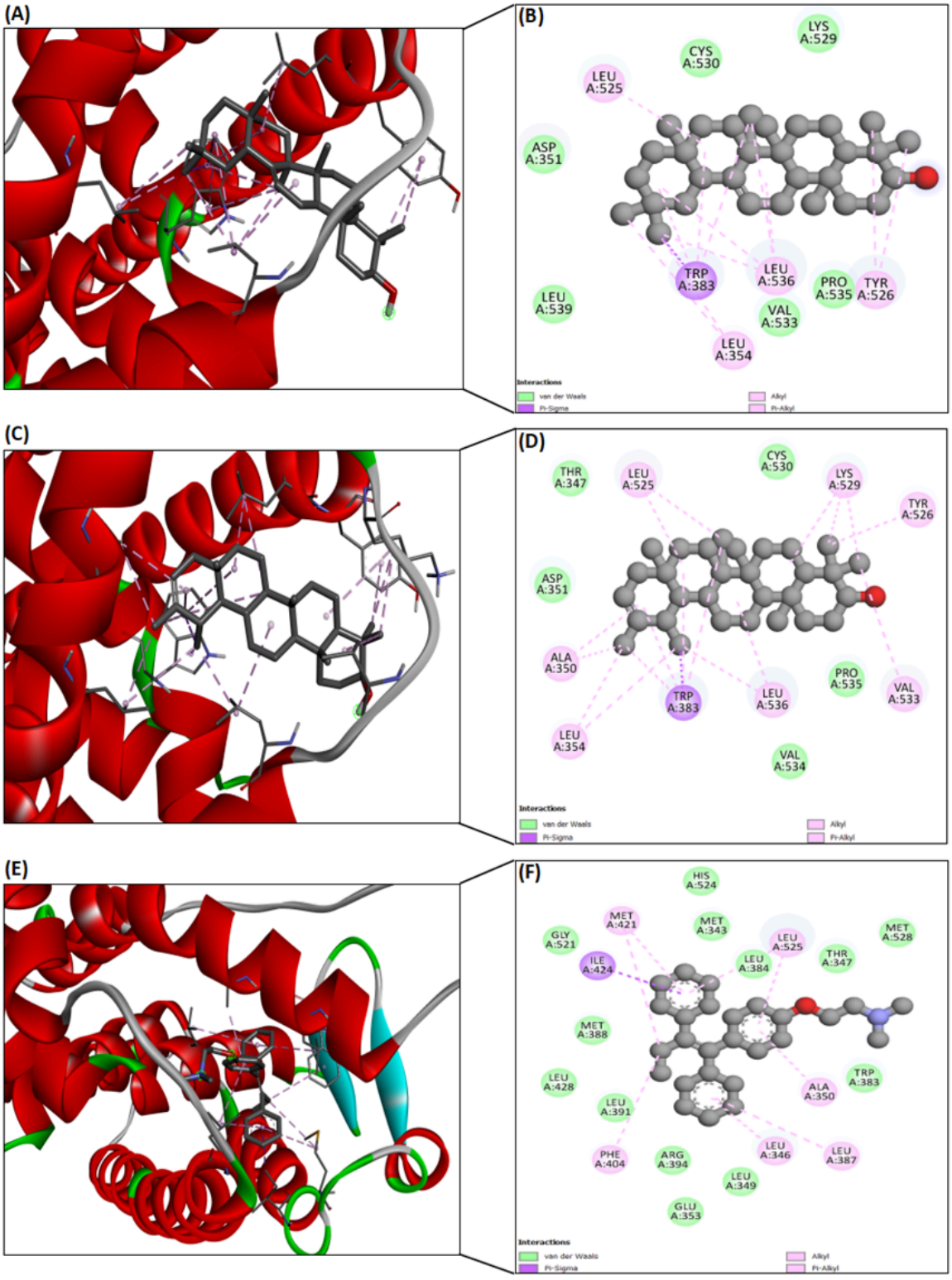

Figure 1

Protein-ligand interaction profile of the docked complex. Where (**A**) represents the interaction between 3ERT and Beta-Amyrin (PubChem CID: 73145) whereas (**B**) shows non bonded interaction between them. On the other hand, (**C**) represents the interaction between 3ERT and Pseudotaraxasterol (PubChem CID: 12305110) whereas (**D**) shows non bonded interaction between them. (**E**) represents the interaction between 3ERT and control (PubChem CID: 2733526) whereas (**F**) shows non bonded interaction between them.

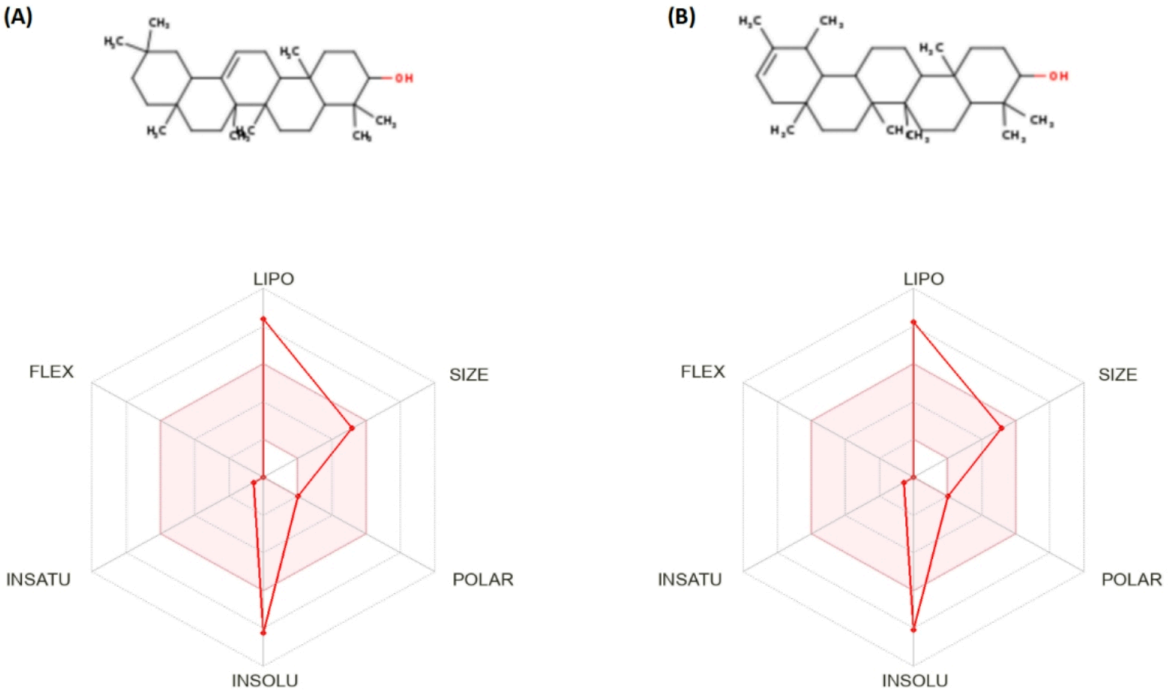

Figure 2

The top two compounds are within colored zone that indicates suitable physio-chemical space for oral bioavailability and show the POLAR (Polarity), INSOLU (Insolubility), INSATU (Instauration), and FLEX (Rotable bond flexibility), LIPO (Lipophilicity), SIZE (Molecular Weight), parameters. (A) Beta-Amyrin (CID 73145), (B) Pseudotaraxasterol (CID 12305110).

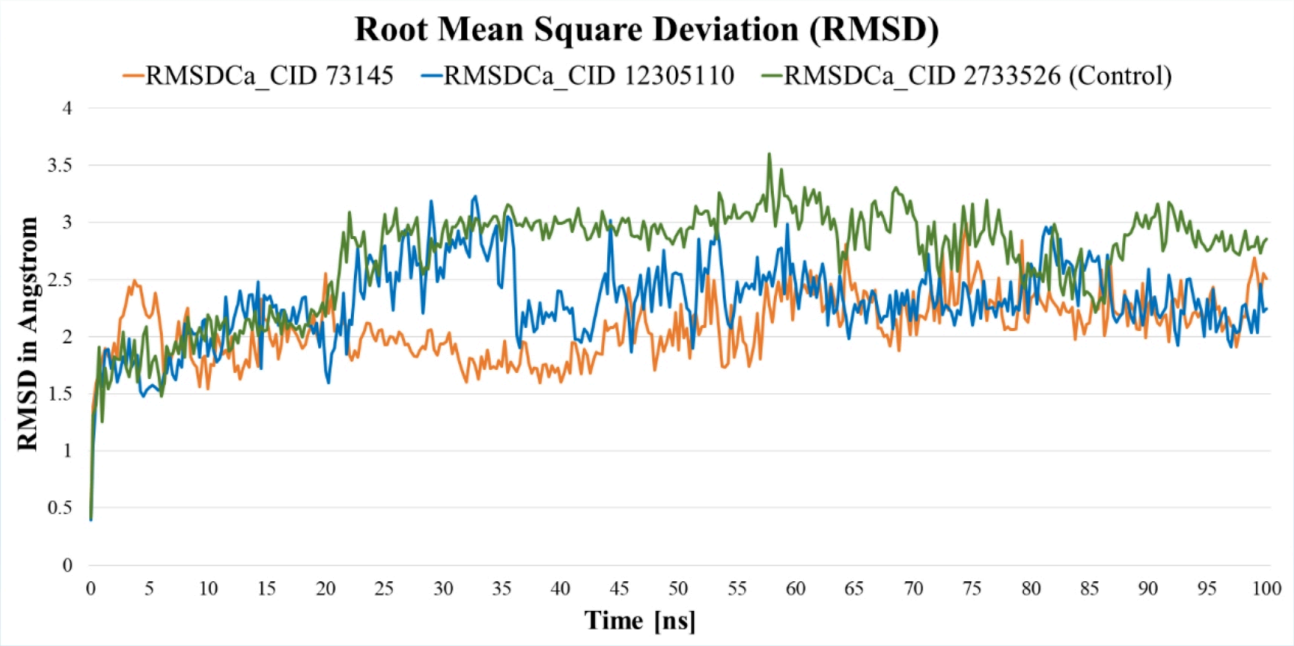

Figure 3

Graphical representation of root mean square deviation (RMSD) for CID 73145 (orange), CID 12305110 (blue), and CID 2733526 (green). The amino acid residue number of 3CERT protein is presented on X axis while Y axis indicates RMSF value in angstrom (Å).

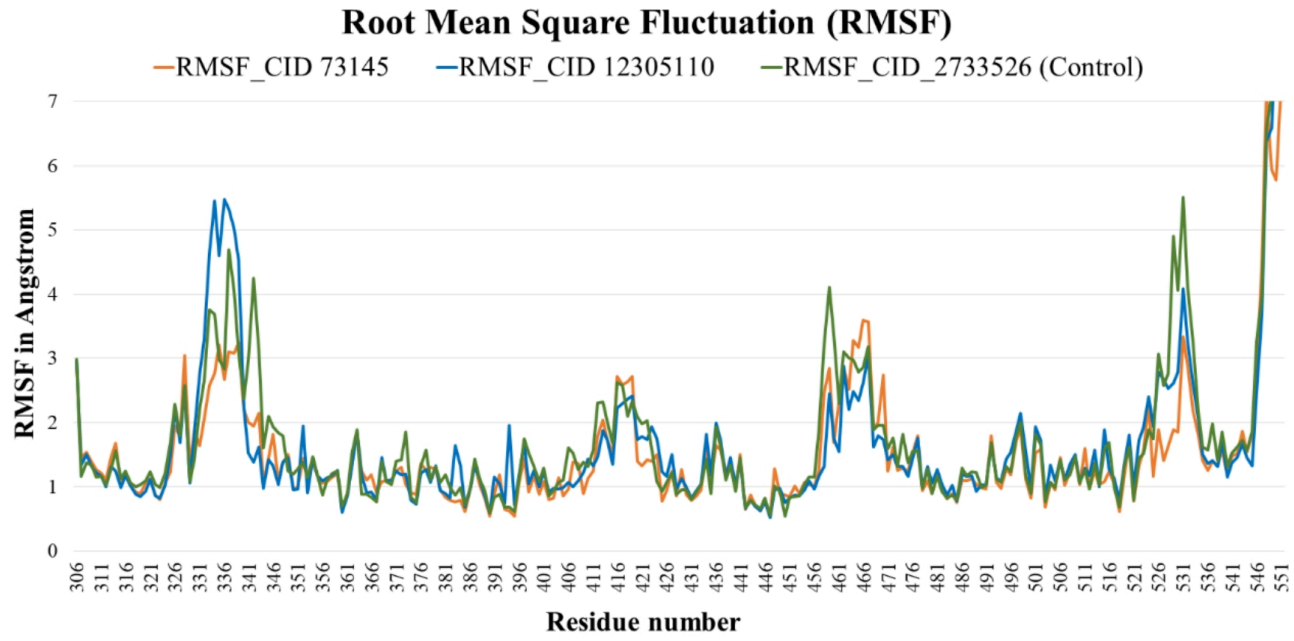

Figure 4

RMSF plot for CID 73145 (orange), CID 12305110 (blue), and CID 2733526 (green). The amino acid residue number of 3ERT protein is presented on X axis while Y axis indicates RMSF value in angstrom (Å).

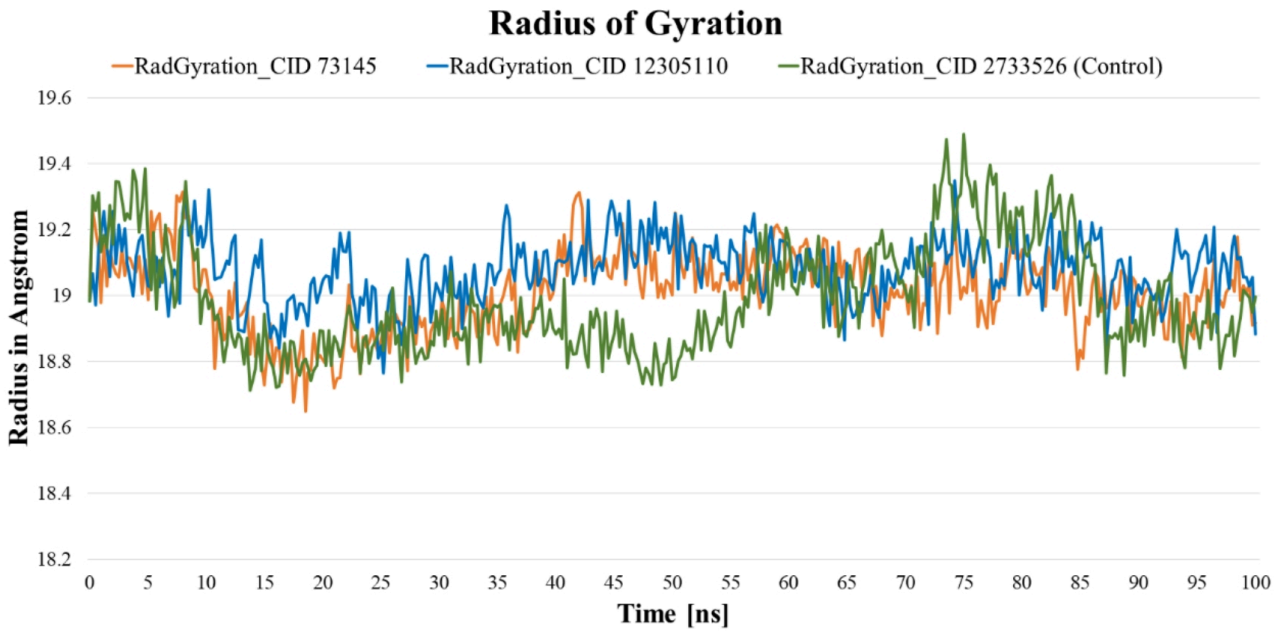

Figure 5

Radiation of gyration (Rg) plot for CID 73145 (orange), CID 12305110 (blue), and CID 2733526 (green). The time frame is presented on X axis while Y axis indicates Rg value in angstrom (Å).

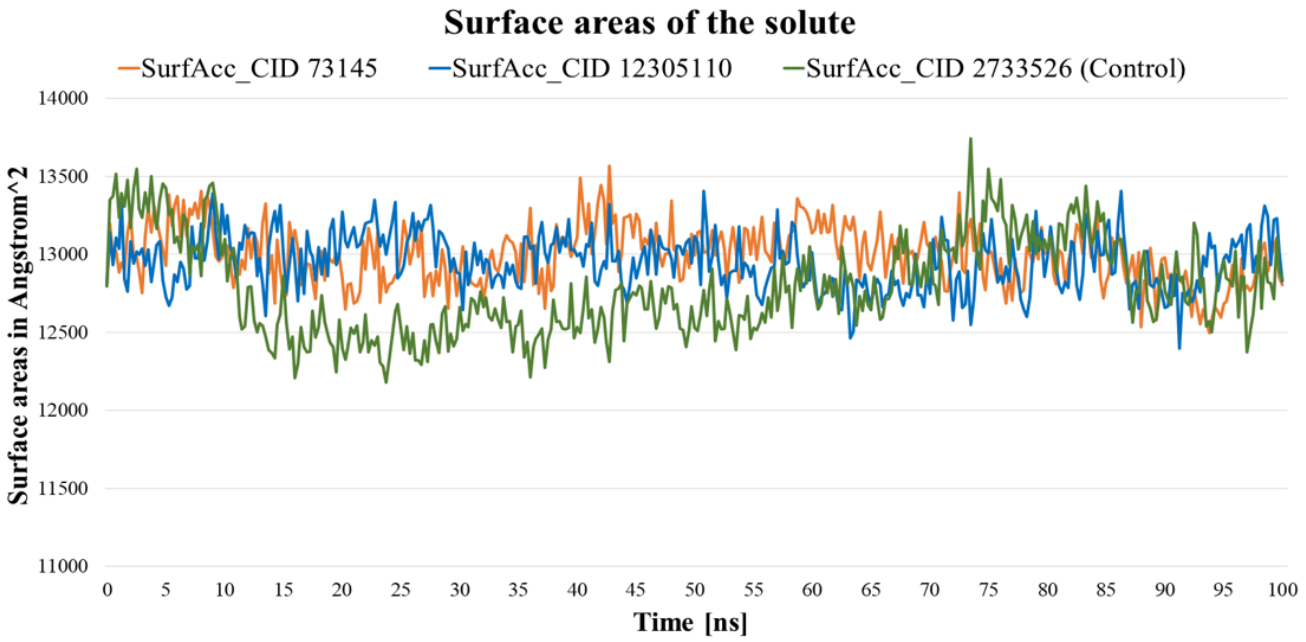

Figure 6

Solvent-accessible surface area (SASA) plot for CID 73145 (orange), CID 12305110 (blue), and CID 2733526 (green). The time frame is presented on X axis while Y axis indicates the SASA value in angstrom (Å).

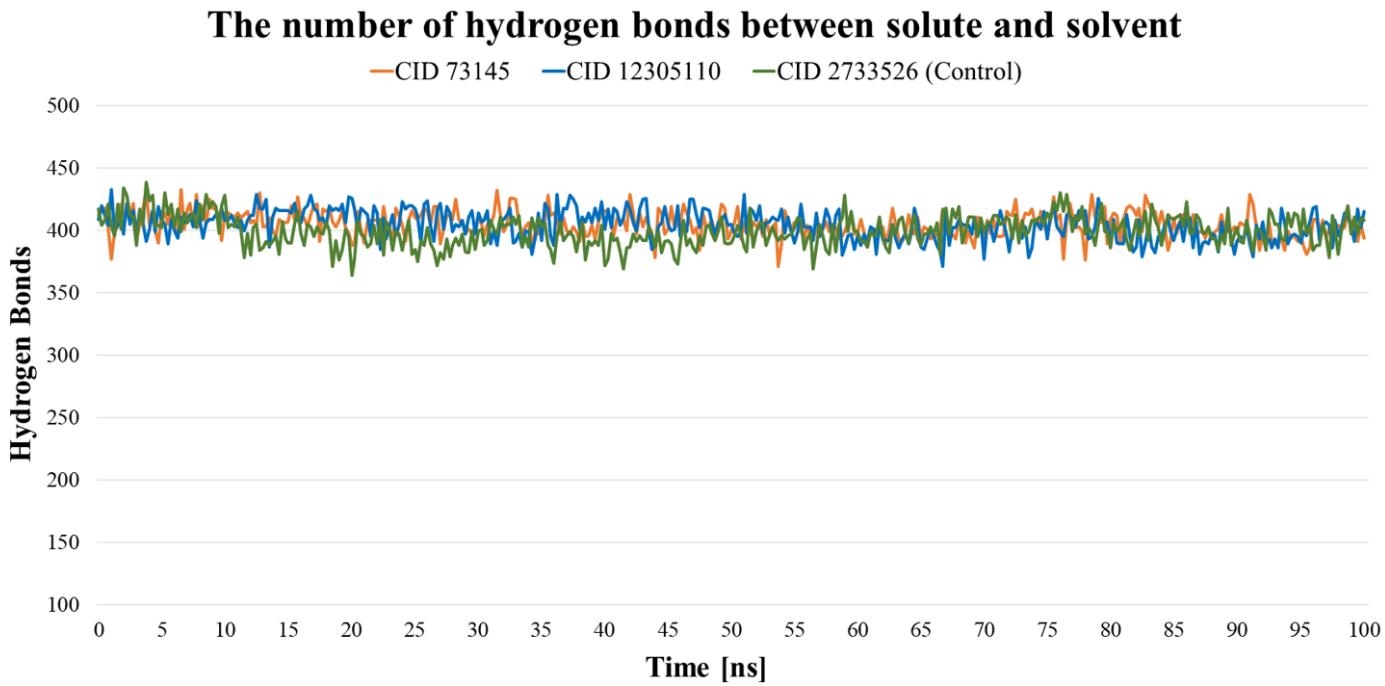

Figure 7

Visual representation of the number of H-bonds between solute and solvents for CID 73145 (orange), CID 12305110 (blue), and CID 2733526 (green). The time frame is presented on X axis while Y axis indicates number of H-bonds.

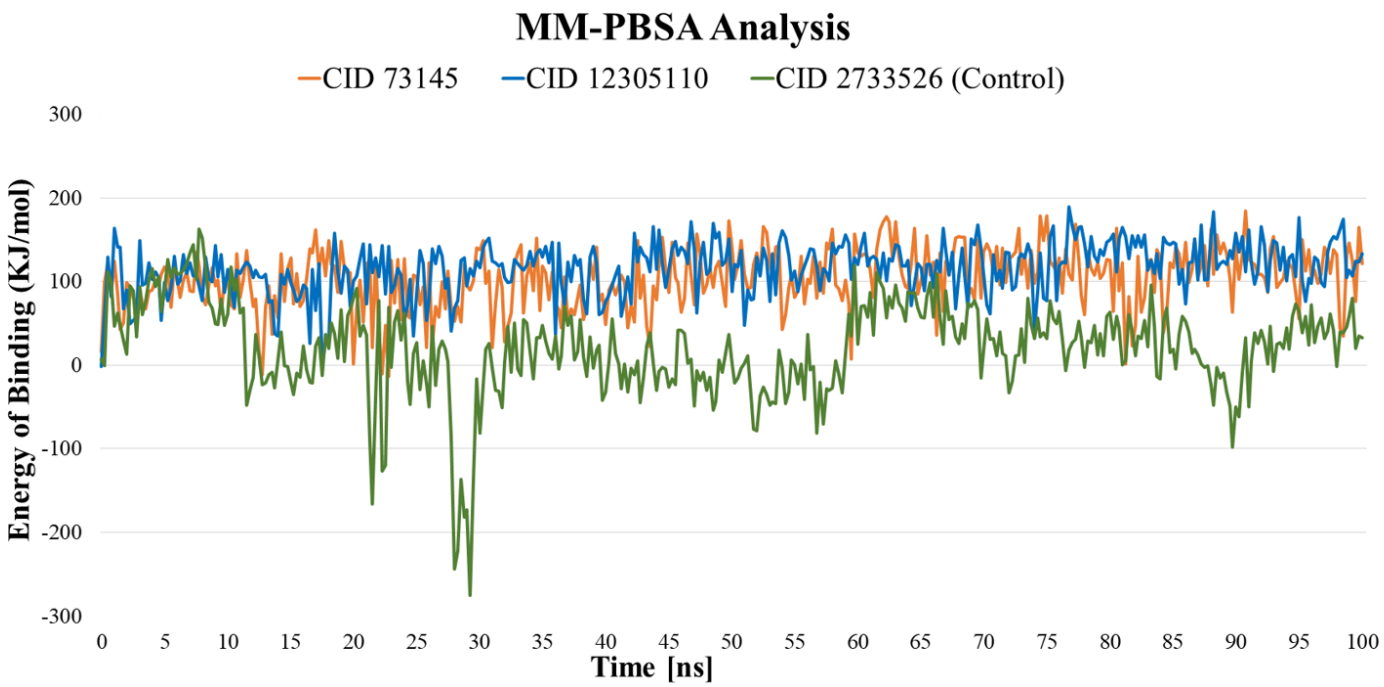

Figure 8

Visual representation of molecular mechanics Poisson Boltzmann surface area (MM/PBSA) for CID 73145 (orange), CID 12305110 (blue), and CID 2733526 (green). The time frame is presented on X-axis while Y-axis indicates the binding energies in kJ/mol.

Supplementary Files

This is a list of supplementary files associated with this preprint. Click to download.

- SupplementaryInformation.docx
- Table1.docx